J. Biochem. **138**, 751–762 (2005)
doi:10.1093/jb/mvi174

Selective Perturbation of the Intravesicular Heme Center of Cytochrome b_{561} by Cysteinyl Modification with 4,4′-Dithiodipyridine

Fusako Takeuchi[1], Hiroshi Hori[2] and Motonari Tsubaki[1,3,*]

[1]Department of Molecular Science and Material Engineering, Graduate School of Science and Technology, Kobe University, Rokkodai-cho, Nada-ku, Kobe, Hyogo 657-8501; [2]Division of Bioengineering, Department of Mechanical Science and Bioengineering, Graduate School of Engineering Science, Osaka University, Machikaneyama-cho, Toyonaka, Osaka 560-8531; and [3]CREST, JST

Received April 17, 2005; accepted September 8, 2005

Cytochrome b_{561} from bovine adrenal chromaffin vesicles contains two hemes *b* with EPR signals at $g_z = 3.69$ and 3.14 and participates in transmembrane electron transport from extravesicular ascorbate to an intravesicular monooxygenase, dopamine β-hydroxylase. Treatment of purified cytochrome b_{561} in an oxidized state with a sulfhydryl reagent, 4,4′-dithiodipyridine, caused the introduction of only one 4-thiopyridine group per b_{561} molecule at either Cys57 or Cys125. About half of the heme centers of the modified cytochrome were reduced rapidly with ascorbate as found for the untreated sample, but the final reduction level decreased to ∼65%. EPR spectra of the modified cytochrome showed that a part of the $g_z = 3.14$ low-spin EPR species was converted to a new low-spin species with $g_z = 2.94$, although a considerable part of the heme center was concomitantly converted to a high-spin $g = 6$ species. Addition of ascorbate to the modified cytochrome caused the disappearance or significant reduction of the EPR signals at $g_z = 3.69$ and 3.14 of low-spin species and at $g = 6.0$ of the high-spin species, but not for the $g_z \sim 2.94$ species. These results suggested that the bound 4-thiopyridone at either Cys57 or Cys125 affected the intravesicular heme center and converted it partially to a non–ascorbate-reducible form. The present observations suggested the importance of the two well-conserved Cys residues near the intravesicular heme center and implied their physiological roles during the electron donation to the monodehydroascorbate radical.

Key words: ascorbate, cysteine residue, cytochrome b_{561}, EPR, MALDI-TOF-MS, 4-PDS, stopped-flow rapid-scan spectroscopy, transmembrane electron transfer.

Abbreviations: EPR, electron paramagnetic resonance; AsA, ascorbate; MDA, monodehydroascorbate; 4-PDS, 4,4′-dithiodipyridine; 2-PDS, 2,2′-dithiopyridie; MALDI-TOF, matrix-assisted laser desorption/ionization-time of flight; 4-TP, 4-thiopyridine; DEPC, diethylpyrocarbonate.

In neurosecretory vesicles, such as adrenomedullary chromaffin vesicles and pituitary neuropeptide secretory vesicles, intravesicular ascorbate (AsA) (about 20 mM) functions as the electron donor for copper-containing monooxygenases including dopamine β-hydroxylase and peptidyl-glycine α-amidating monooxygenase (*1–3*). These monooxygenase reactions produce the monodehydroascorbate (MDA) radical within the vesicles by the univalent oxidation of AsA (*4*). Neither AsA nor the MDA radical can pass through vesicle membranes due to their intrinsic negative charge, although dehydroascorbate, the fully-oxidized neutral form, can diffuse through membranes (*5–7*). It is believed that the intravesicular MDA radical is reduced back to AsA by membrane-spanning cytochrome b_{561}, and the oxidized cytochrome b_{561} is subsequently reduced by AsA on the extravesicular side (about 5 mM). Thus, cytochrome b_{561} acts as a neuroendocrine-specific transmembrane electron transporter (*8–10*). Midpoint potentials for AsA/MDA radicals and for MDA radical/dehydroascorbate are +330 mV and –210 mV, respectively (*11*), and are suitable for such specific chemistry to occur.

Cytochrome b_{561} is a highly hydrophobic hemoprotein (*12*, *13*) with a molecular mass of 29 kDa (*12*, *14*). We have established that purified cytochrome b_{561} contains two distinct heme *b* centers, with one heme *b* showing a usual low spin EPR signal ($g_z = 3.14$) and the other exhibiting a highly anisotropic low spin EPR signal ($g_z = 3.70$) (*15*), as observed in chromaffin vesicle membranes (*16*). The presence of two distinct heme centers in cytochrome b_{561} was verified very recently based on the expression of the bovine cytochrome in yeast and insect cells (*17*). Based on the deduced amino acid sequences of cytochrome b_{561} from various animals (*18–21*), we have proposed a structural model of cytochrome b_{561} (*22*) by extending the model of Degli Esposti (*23*). In our model (Fig. 2), there are two conserved sequences, the first (^{69}ALLVYRVFR^{77}) located on the extravesicular side of an α-helical segment, and the second (^{120}SLHSW^{124}) in an intravesicular loop connecting two α-helical segments (*22*). We proposed further that the two hemes *b* were likely to be located on opposite sides of the vesicular membrane in close contact with these

*To whom correspondence should be addressed. E-mail: mtsubaki@kobe-u.ac.jp

putative binding sites (for the extravesicular AsA and intravesicular MDA radical, respectively) (Fig. 2) (*22*).

Our pulse radiolysis analysis of cytochrome b_{561} indicated that the two heme *b* centers had distinct roles in electron donation to the MDA radical and electron acceptance from AsA, respectively (*24*). We found that the electron-accepting ability from AsA was selectively destroyed by treating oxidized cytochrome b_{561} with diethylpyrocarbonate (DEPC) (*25*). However, the electron-donating activity from the reduced heme *b* center to the MDA radical was retained after the treatment (*25*). We found that two fully conserved histidyl residues (His88 and His161), possible heme axial ligands on the extravesicular side, and one well-conserved lysyl residue (Lys85) were selectively *N*-carbethoxylated upon treatment with DEPC (*25*). The electron-accepting ability from AsA, however, could be protected by the presence of AsA during the DEPC treatment, suggesting that the AsA-binding site is on the extravesicular side (*26*, *27*). We observed that the purified cytochrome b_{561} showed a sigmoidal shape upon redox titration, consistent with the presence of two heme *b* redox centers with slightly different midpoint potentials (+170 and +60 mV) (*28*), and that the treatment of oxidized cytochrome b_{561} with DEPC caused a downshift of the midpoint potential for the lower redox component (*26*). All these pieces of evidence seemed to favor our six trans-membrane helices model containing two heme *b* centers (*22*).

Recently, a new member of cytochrome b_{561} family was identified in plasma membranes of duodenal enterocytes (*29*, *30*). Dcytb (for duodenal cytochrome b_{561}) was reported to be responsible for the physiological ferric reductase activity in duodenal mucosa and an important element in the iron absorption pathway (*29*). Cytochrome b_{561} and Dcytb share a similar membrane topology and potential histidyl heme ligands, indicating that Dcytb might also bind two hemes. Other members of the cytochrome b_{561} family are known to be present in various membranes such as rabbit neutrophils (*31*) and plant cells (*32*–*35*). More distant members of the cytochrome b_{561} family are now emerging (*36*–*39*). Therefore, elucidation of precise structures around the two heme redox centers of cytochrome b_{561} is increasingly important and will be very valuable to clarify the physiological roles of these new transmembrane electron carriers.

During the course of our studies, we noted that there were two well-conserved Cys residues only among a group of cytochromes b_{561} responsible for the electron transfer in neuroendocrine vesicles of higher vertebrates (Fig. 1). The two Cys residues (Cys57 and Cys125 for bovine cytochrome b_{561}) were both considered to lie in close proximity to the heme center on the intravesicular side (Fig. 2), which was

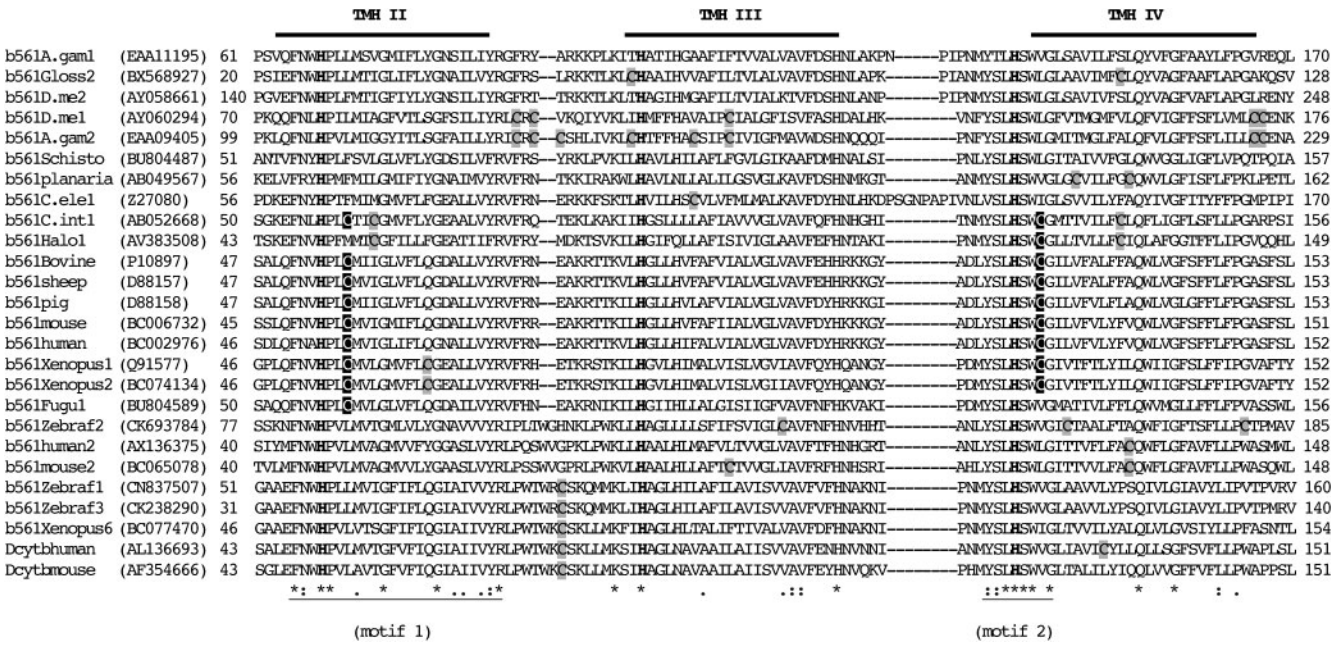

Fig. 1. **Multiple sequence alignment of the core domain of cytochrome b_{561} from animal species.** Only the sequences belonging to group A (animals/neuroendocrine) (*37*) are shown. Group A consists of cytochromes b_{561} residing in neuroendocrine vesicles (corresponding to upper 18 sequences and responsible for the transmembrane AsA/MDA electron transfer) and Dcytbs residing in plasma membranes (corresponding to lower 8 sequences and responsible for the transmembrane ferric reductase activity for the acquisition of iron). Fully-conserved residues are indicated by *, whereas well-conserved residues are indicated by : or . beneath the sequences. Fully-conserved His residues (heme axial ligands) are marked in boldface. Well-conserved Cys residues of neuroendocrine cytochromes b_{561} from vertebrates are shown in black-background Cs, whereas other Cys residues are shown in gray-background Cs. The putative transmembrane helices are indicated by a bold line in the uppermost line and are numbered. The well-conserved motifs 1 and 2 (*37*) are indicated by a thin line in the lowest line. In each line of the sequence, the following information is indicated in order: abbreviated name, DDBJ acquisition number in parenthesis, and amino acid sequence of the core region. The abbreviated species names are as follows (in the order of appearance): A.gam, *Anopheles gambiae*; Gloss, *Glossina morsitans morsitans*; D.me, *Drosophila melanogaster*; Schisto, *Schistosoma japonicum*; C.ele, *Caenorhabditis elegans*; C.int, *Ciona intestinalis*; Halo, *Halocynthia roretzi*; Xenopus, *Xenopus laevis*; Fugu, *Fugu rubripes*; Zebraf, *Danio rerio*.

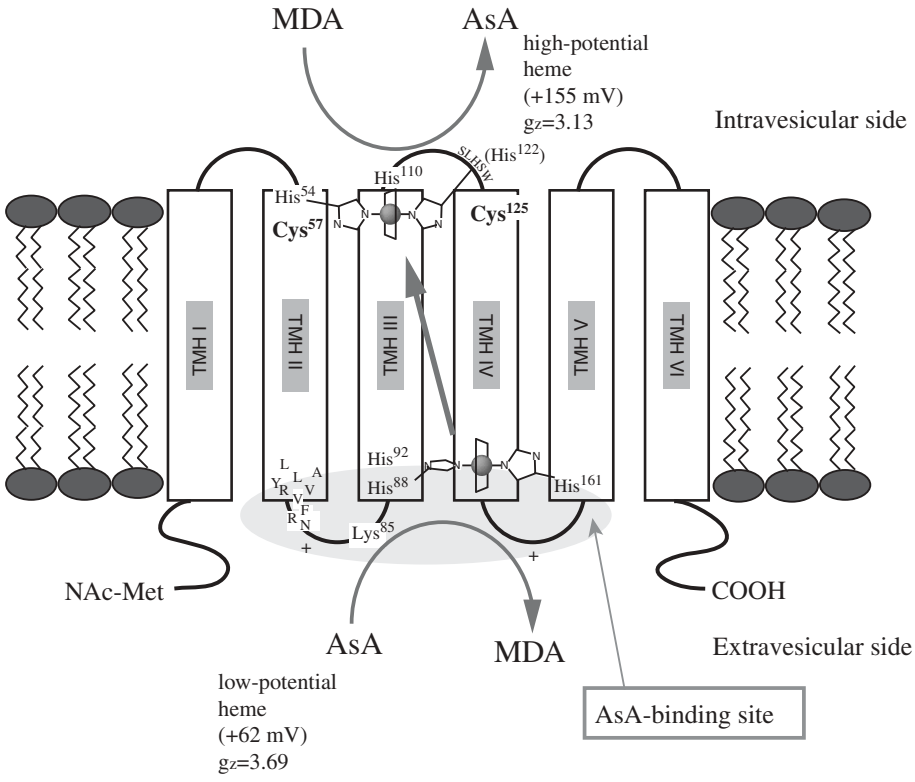

Fig. 2. **Transmembrane structural model of bovine cytochrome b_{561}.** Four totally conserved histidyl residues (His54, His88, His122, and His161) and two well-conserved sequences (^{69}ALLVYRVFR^{77} and ^{120}SLHSW^{124}) are indicated based on Ref. *22*. His54 and His122 are likely the heme axial ligands on the intravesicular side, whereas His161 and His88 are considered as the heme axial ligands on the extravesicular side. The heme on the intravesicular side functions to donate electrons to MDA radical, whereas the heme on the cytosolic site functions to accept electrons from AsA. Two Cys residues (Cys57 and Cys125) [well-conserved among neuroendocrine cytochromes b_{561} from higher vertebrate species (*37*)] are indicated just below the two heme axial ligands (His54 and His122) on the intravesicular side, and are likely to have an important role(s) in electron donation to the MDA radical.

indicative of some physiological roles. The fraction of Cys residues is very small in proteins (1.44% of all amino acid residues) (*40*). However, Cys residues have many important functions in proteins by utilizing their two different chemical structures; disulfide-bonding half-cystine (Cys-SS) and free cysteine (Cys-SH). A covalent disulfide bond (-SS-) is formed between two half-cystine residues in close proximity with each other by an oxidation reaction and contributes to a protein's tertiary structure. However, because of the reduced condition of the intracellular milieu, it is very rare to find the formation of a disulfide bond in intracellular proteins. In contrast, the sulfhydryl groups (-SH) of free Cys residues are polarized and sometimes, in a thiolate form, participate in metal binding, as proximal axial ligands for the heme iron in dioxygen-activating hemoproteins (cytochromes P450 and nitric oxide synthases) (*41*) or as ligands for the iron-sulfur clusters (*42*). Further, in the enzyme ribonucleotide reductase, a Cys residue serves as a site for the formation of a transient thiyl radical to support the catalysis at the diiron-oxo active site (*43*). To clarify the chemical structure and roles of Cys residues in proteins and enzymes, reagents specific for sulfhydryl groups (-SH) are widely used (*44–47*).

The present study focused on the nature of the two conserved Cys residues and the effect of their specific modification with a sulfhydryl-specific reagent, 4,4′-dithiodipyridine (4-PDS), on the intravesicular heme center, where the electron donation to MDA radical is expected to occur. We conducted an EPR spectroscopic analysis together with an AsA-reduction assay to evaluate the structure around the intravesicular heme moiety and the physiological roles of the conserved Cys residues.

MATERIALS AND METHODS

Purification of Cytochrome b_{561}—Cytochrome b_{561} was purified as described previously (*15*). The purity of cytochrome b_{561} was determined from its visible absorption spectrum, heme content analysis, and SDS–polyacrylamide gel electrophoresis (*15*). The concentration of cytochrome b_{561} was determined using a millimolar extinction coefficient of 267.9 mM^{-1} cm^{-1} at 427 nm in the reduced form (*15*).

Modification of Cytochrome b_{561} with 4,4′-Dithiodipyridine—The concentrated cytochrome b_{561} solution was acidified to pH 6.5 by adding 0.5 M sodium-phosphate buffer (pH 6.0) and was oxidized by step-wise addition of potassium ferricyanide solution (100 mM). Complete oxidation was checked by visible absorption spectroscopy. The oxidized cytochrome b_{561} was gel-filtered through a PD-10 column (Amersham Pharmacia Biotech) equilibrated with 50 mM potassium-phosphate buffer (pH 6.5) containing 1.0% (w/v) octyl β-glucoside (buffer A), and then diluted with the same buffer to an appropriate concentration. The diluted sample was treated with various concentrations of 4,4′-dithiopyridine (4-PDS) according to a following procedure.

Optical quartz cells (light path, 1.0 cm) containing 1.0 ml of diluted cytochrome b_{561} solution (typically 1.0 μM) were placed in sample and reference cell holders of a Shimadzu UV-2400 PC spectrophotometer equipped with a thermostatted cell holder connected to a thermobath (RC6 CS, Lauda). Temperature was maintained at 20°C during the whole measurement. The base line was recorded before the reaction started. An appropriate amount of 4-PDS solution (30 mM in buffer A) and an equal amount of buffer A

were added to the sample and the reference cells, respectively. The final concentration of 4-PDS was around 40 μM unless otherwise indicated. The spectral changes were recorded from 200 to 700 nm at 15-min intervals at 20°C.

After cessation of the reaction, or at an appropriate time, the 4-PDS–treated samples were gel-filtered through a PD-10 column equilibrated with buffer A to remove unreacted 4-PDS. The 4-PDS–treated cytochrome b_{561} samples were then analyzed for the reactivity with AsA with a Shimadzu UV-2400 PC spectrophotometer. Finally, the sample was fully reduced with sodium dithionite, and its absorption spectrum was recorded to check the integrity of the heme moiety. The reduction level was analyzed with the absorbance at both 561 (α-band) and 427 nm (Soret band) by normalizing against the reduction level of the dithionite-reduced state.

Digestion of Cytochrome b_{561} with Trypsin or V8 Protease—Digestion of cytochrome b_{561} sample was started by addition of TPCK-treated trypsin (from bovine pancreas, Sigma Chemical Co., St. Louis, MO) (final 0.76 μM) or V8 protease (from *Staphylococcus aureus* V8, Wako Pure Chemical Industries, Ltd., Osaka, Japan) (final 1.48 μM), to the oxidized cytochrome b_{561} (control) or the 4-PDS–treated cytochrome b_{561} (~50 μM) in buffer A at room temperature, as previously described (*26*, *25*). The extent of the digestion was checked by mass spectrometric analysis with an appropriate interval.

MALDI-TOF Mass Spectrometry—Mass spectrometric analyses were carried out on a Voyager RP mass spectrometer (Applied Biosystems) using a 20 kV accelerating voltage as previously described (*26*, *25*). The samples were run in a linear mode. The protein solutions were diluted 1:9 (v/v) with a matrix solution, 3,5-dimethoxy-4-hydroxycinnamic acid (Aldrich, Gillingham, England), 50 mg/ml in 30% acetonitrile in 0.3% TFA. The mixtures (typically 1.0 μl) were deposited on the sample plate and allowed to air-dry before analysis. Insulin (bovine, 5,733.69 Da), thioredoxin (*Escherichia coli*, 11,673.68 Da), and apomyoglobin (horse, 16,951.56 Da) were used as external standards for a higher molecular weight region. Angiotensin I (1,296.51 Da), ACTH (clip 1–17, 2,093.46 Da; clip 18–39, 2,465.72 Da; clip 7–38, 3,659.19 Da), and insulin (bovine, 5,733.69 Da) were used as external standards for a lower molecular weight region. The search for the corresponding fragments in the amino acid sequence of cytochrome b_{561} was carried out using the program GPMAW (v 3.15) (Lighthouse Data, Odense M, Denmark). The molecular masses of all polypeptides measured matched the theoretical ones, obtained from the bovine cytochrome b_{561} amino acid sequence (*18*), within an accuracy of 0.1% or better.

Stopped-Flow Rapid-Scan Measurements—Rapid kinetic measurements were carried out using an RSP-100-03DR stopped-flow rapid-scan spectrometer (Unisoku Co. Ltd., Osaka, Japan). One chamber of the apparatus contained oxidized cytochrome b_{561} (2.0 μM or indicated in the text) in 50 mM sodium acetate (pH 5.5) or 50 mM potassium-phosphate (pH 6.5) buffer containing 1.0% octyl β-glucoside. The other chamber contained a test concentration of sodium ascorbate (AsA) (2, 4, 8, 16 mM) in the same buffer. The temperature of both chambers and the sample holder was maintained at 20°C with a connection to a thermo-bath (Tokyo Rikakikai Co., Ltd., Model NCB-1200). The mixing was carried out with 1:1 (v/v) ratio. Reduction of cytochrome b_{561} was followed spectrophotometrically either by absorbance change at 427 nm using a photomultiplier (single wavelength mode) or by multiple wavelengths (rapid-scan mode; ~360–640 nm) using a photodiode array (512 channels). Data points were collected in every 5 msec during the 10-s measurements for the singe-wavelength mode (total 2,000 data points). During the measurements with the rapid-scan mode, spectra were obtained in every 120 ms (with a 1-ms exposure time) for 1 min. The time-courses of the absorbance change at 427 nm were fitted by use of a non-linear least-squares method of a built-in software of the apparatus with a single (or a linear combination of) exponential decay equations.

Measurements of EPR Spectra—The oxidized cytochrome b_{561} samples (either control or 4-PDS–treated in the oxidized form) in 50 mM sodium-phosphate buffer (pH 6.5) containing 1.0% (w/v) octyl β-glucoside were concentrated to about 230 μM with a 50-ml Amicon concentrator fitted with a membrane filter (Millipore PTTK04310; pore size 30,000 NMWL). The concentrated samples were introduced into EPR tubes and frozen in liquid nitrogen (77 K). To obtain AsA-reduced forms, a small volume of concentrated AsA solution was added aerobically to the oxidized forms of cytochrome b_{561} (final AsA concentration, 20 mM). The samples were then left at room temperature for 30 min to insure complete equilibrium, transferred to EPR tubes, and then frozen in liquid nitrogen. EPR measurements were carried out at X-band (9.23 GHz) microwave frequency with a Varian E-12 EPR spectrometer with 100-kHz field modulation. An Oxford flow cryostat (ESR-900) was used for the measurements at cryogenic temperatures (from 5 to 20 K). The microwave frequency was calibrated with a microwave frequency counter (Takeda Riken Co., Ltd., Model TR5212). The magnetic field was determined with an NMR field meter (Echo Electronics Co., Ltd., Model EFM 2000AX). The accuracy of the g-values was approximately ±0.01.

RESULTS

Free Sulfhydryl Determination—Since the mature form of bovine cytochrome b_{561} contains two Cys residues (Cys57 and Cys125) per molecule based on the deduced amino acid sequence (*18*), we first analyzed whether both of these residues react with sulfhydryl reagents in the native conformation in the presence of a mild detergent, β-octyl glucoside. Two kinds of sulfhydryl reagents, 2-PDS and 4-PDS, were employed. It was expected that, upon the thio-disuphide exchange reaction with a free Cys residue(s), either 2-thiopyridone (A_{max} = 343 nm; ε_{mM} = 7.06 mM^{-1} cm^{-1}) or 4-thiopyridone (A_{max} = 324 nm; ε_{mM} = 24.59 mM^{-1} cm^{-1}) would be produced and released. Therefore, the increase in absorbance in the ultraviolet region was analyzed. Results are shown in Table 1. We found that 4-PDS had a slightly higher reactivity toward the Cys residues of cytochrome b_{561}. With a 2-h incubation at 20°C at pH 6.5, about 0.6 Cys residue was modified with 2-PDS, whereas 4-PDS–treatment caused the introduction of about 0.9 thiopyridine (4-TP) group per molecule (Table 1). Since the absorbance intensity at 343 nm for the 2-thiopyridone was too small to analyze the extent of

Table 1. **Reactivity of Cys residues in oxidized cytochrome b_{561} with either 2-PDS or 4-PDS.**

Reaction time	pH	Average number of residues modified/molecule	SD
2-PDS (40 μM)			
2 h	pH 6.0	0.503	± 0.036
	pH 6.5	0.616	± 0.007
4-PDS (40 μM)			
2 h	pH 6.0	0.682	–
	pH 6.5	0.929	± 0.005
	pH 6.5	1.087	± 0.166

Reactions of oxidized cytochrome b_{561} with 2-PDS or 4-PDS were conducted as described in the text. SD, standard deviation (3 independent measurements).

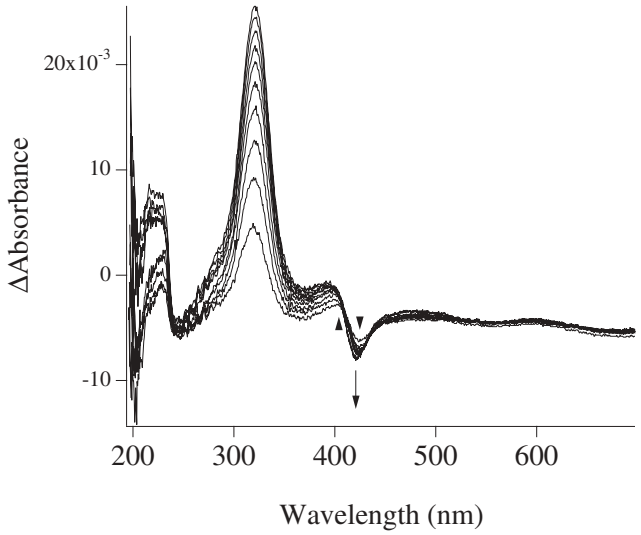

Fig. 3. **Spectral changes of oxidized cytochrome b_{561} associated with the release of 4-thiopyridone upon thio-disulphide exchange reaction at two Cys residues.** The spectral changes are shown as difference spectra with the spectrum of oxidized cytochrome b_{561} (1.0 μM) just after the addition of 4-PDS (40 μM) as the base line. The increase in absorbance at 324 nm is due to the release of 4-thiopyridone upon thio-disulphide exchange reaction between the free -SH group of the two Cys residues and the lipophilic reagent, 4-PDS. Changes in absorbance around 420 nm are ascribable to the heme moieties of cytochrome b_{561}. Two kinds of spectral changes occurred successively. The first one was a "derivative-type" spectral change with a minimum at 425 nm and a maximum at 405 nm (indicated by arrow heads) in the difference spectra. The second type showed a minimum at 422 nm (indicated by an arrow), but the maximum in the difference spectra became obscured, indicating a conversion of the low-spin heme center to a new perturbed state(s).

the suflhydryl modification precisely, we decided to use 4-PDS, hereafter.

Typical difference absorbance changes after the addition of 4-PDS to the oxidized cytochrome b_{561} are shown in Fig. 3. There was a steady and gradual time-dependent increase in absorbance at 324 nm, in addition to the spectral changes around 420 nm. The latter indicated that the heme absorption spectrum was perturbed upon modification of either one of or both of the two Cys residues with 4-PDS. Longer incubation time (up to 20 h) at 20°C showed a saturation behavior of the reaction, approaching to the final modification level of 1.6 Cys residues per

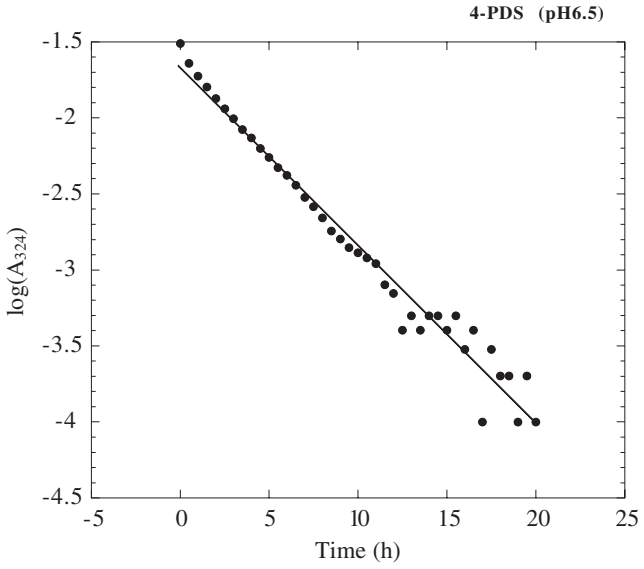

Fig. 4. **A typical time course of the reaction of oxidized cytochrome b_{561} with 4-PDS.** The increase in the absorbance at 324 nm was plotted against time up to 20 h in a semi-logarithmic scale. The plot was simulated as a linear line with a least-square regression method, suggesting that the reaction occurred with quasi first-order reaction kinetics (k = 0.269 h^{-1}) for the entire period of incubation (20 h). Reaction conditions: 20°C at pH 6.5. Other details are described in the text.

cytochrome b_{561} molecule. This result indicated that both of the Cys residues existed in the free cysteine (Cys-SH) state and, therefore, there was no -SS- disulfide bond in cytochrome b_{561}. To analyze the difference in the reactivity of the two Cys residues kinetically, the absorbance changes at 324 nm were plotted in a semi-logarithmic scale, as shown in Fig. 4. The plot showed a straight line, indicating that the reactivities of the two Cys residues were indistinguishable from each other. We routinely prepared the 4-PDS-treated cytochrome b_{561} sample with 5-h incubation at pH 6.5 at 20°C. Under these conditions, about 1.0 Cys group was modified with 4-PDS based on the release of a 4-thiopyridone group (Table 1).

MALDI-TOF MS Analysis of the 4-PDS–Treated Cytochrome b_{561}—We next analyzed the exact modification sites upon the 4-PDS treatment using MALDI-TOF MS analysis. We used a sample in which about one molecule of 4-thiopyridine (4-TP) per cytochrome b_{561} molecule was introduced. The MALDI-TOF analysis of whole cytochrome b_{561} molecule after the modification with 4-PDS was unsuccessful due to the broadening of the molecular mass peak (data not shown). The 4-PDS–treated cytochrome b_{561} (or untreated control sample) was digested with either TPCK-treated trypsin or *Staphylococcus aureus* V8 protease at room temperature, and the digests were analyzed directly. Introduction of a 4-thiopyridine (4-TP) group could be identified with an increase in mass by 109.16 (m/z), compared to unmodified peptides (*26*, *25*). Analyses of the V8 protease digests showed that both Cys57 and Cys125 were modified with 4-PDS (Fig. 5, A and B). The unmodified peptide 47–79 (cleaved with V8 protease) and its 4-PDS–modified peptide (47–79+4TP) appeared with almost the same intensities (Fig. 5A), suggesting that about a half of the Cys57 residue was modified with 4-PDS. In a higher mass region,

there was another group of peptides containing Cys125, such as peptides 80–182, 93–81, 109–182, and 118–182 (Fig. 5B). An unmodified peptide 80–182 was accompanied by its 4-PDS–modified peptide (80–182+4TP) with about a 6:4 intensity ratio. Other related unmodified peptides, such as 93–81, 109–182, and 118–182, also had their 4-PDS–modified peptides with almost the same intensity ratios (Fig. 5B). These results suggested that the modification

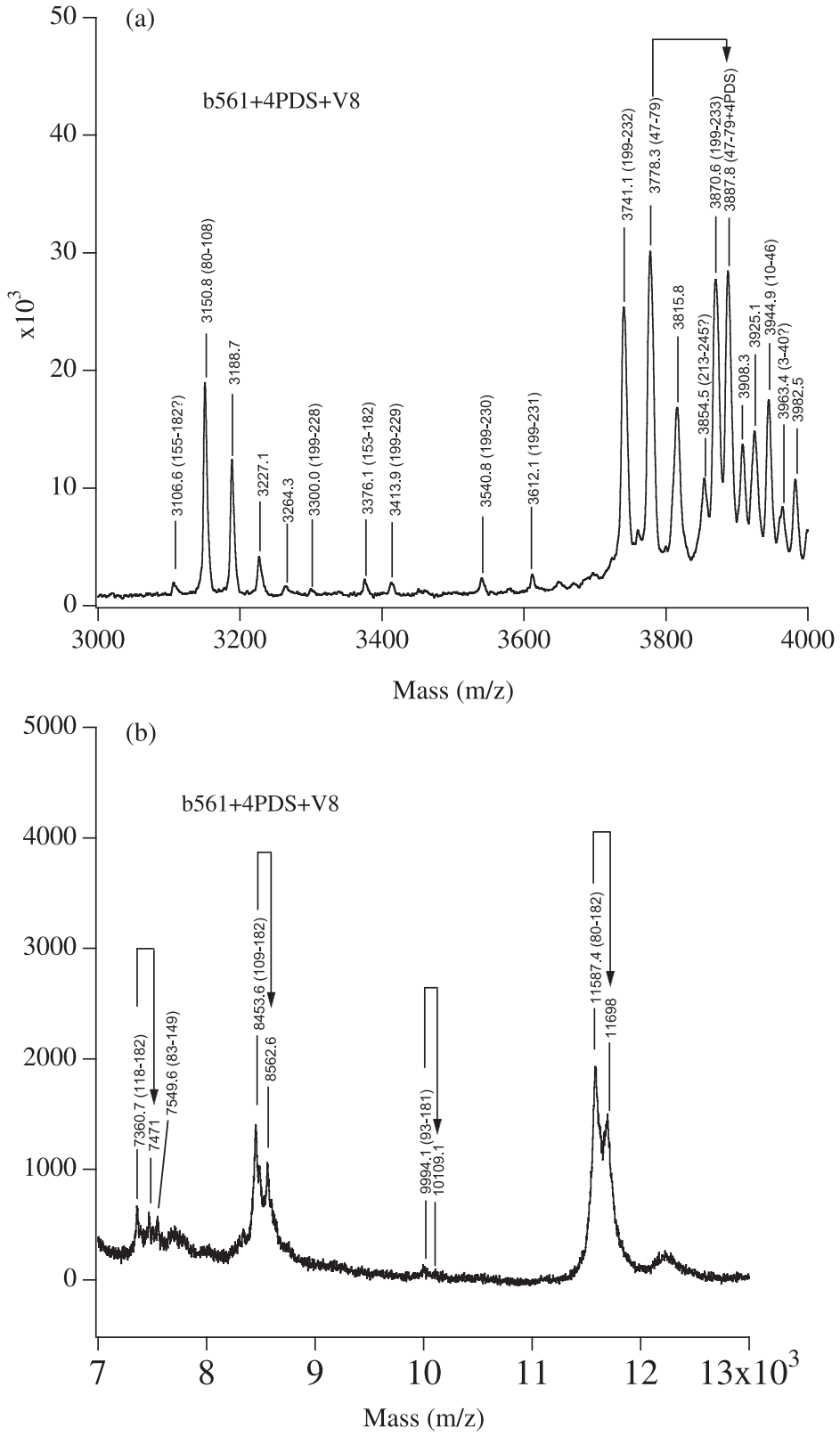

Fig. 5. **MALDI-TOF mass spectra of V8 protease (panel A and B) and tryptic (panel C) digests obtained from the untreated (trace a) and the 4-PDS (40 μM)–treated cytochrome b_{561}.** V8 protease or tryptic digests were obtained as described in the text. A mixture of the polypeptides was directly analyzed with MALDI-TOF mass spectrometry. Other conditions are described in the text. The number for each peak indicates observed mass (m/z) followed by the assignment of each polypeptide to a range of amino acid residues. The peaks corresponding to polypeptides containing 4-thiopyridine (4-TP) group are indicated by arrows, and the introduction of the group into the polypeptide is indicated (*e.g.*, "+4TP"). Peaks indicated by an asterisk are due to $[M+K^+]$ species.

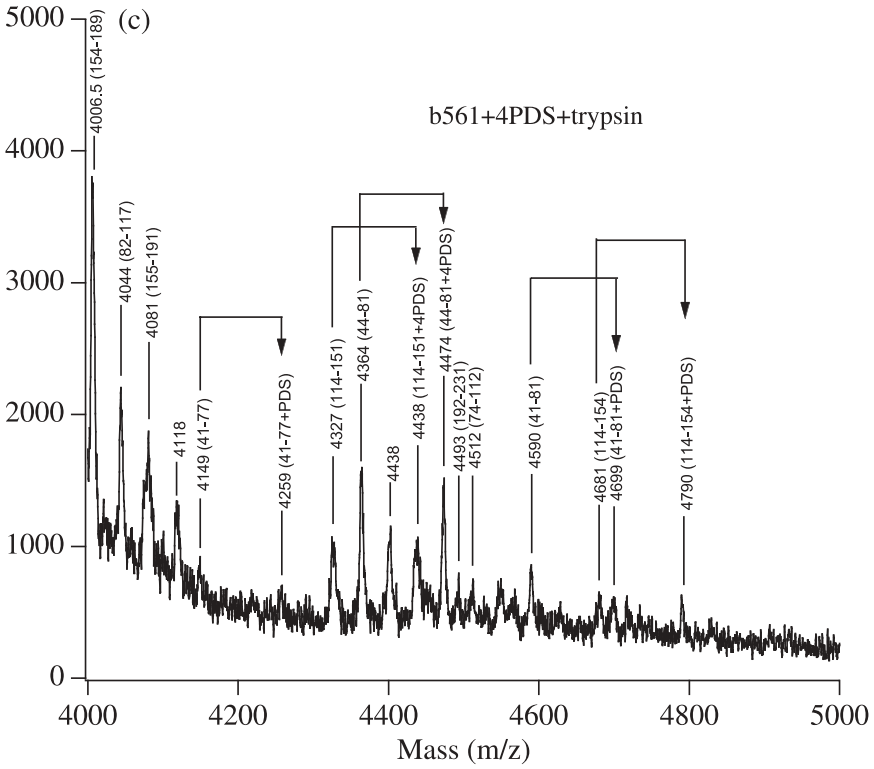

Fig. 5. Continued.

level at Cys125 was slightly less than that of Cys57. To confirm the reactivity of the two Cys residues with 4-PDS, we analyzed tryptic peptides of the 4-PDS–treated cytochrome b_{561}. The result showed that indeed both Cys57 and Cys125 were modified to similar extents, about a half of each residue being modified with the 4-thiopyridine (4-TP) group (Fig. 5C). For Cys57, unmodified peptides 41–81, 44–81, and 41–77 showed accompanying 4-PDS–modified peptides with similar intensities, respectively. For Cys125, an unmodified peptide 114–151 showed its 4-PDS–modified peptide (114–151+4TP) with a similar intensity (Fig. 5C).

Effects of the 4-PDS Modification on the Reactivity with AsA—Effects of the 4-PDS modification on the electron transfer reaction from AsA to the oxidized heme center were analyzed spectrophotometrically. For a control sample (without 4-PDS treatment), both of the heme centers were reduced rapidly upon addition of AsA (final 2.0 mM) with the final reduction level of around 85% (Fig. 6A, line a; Fig. 6C, line b), as previously reported (*48*, *26*, *25*). Treatment of oxidized cytochrome b_{561} with 4-PDS did not cause any appreciable influence on the fast reactivity towards AsA (Fig. 6A, line b), but the final reduction level of the heme center was inhibited significantly (decreased to about 60%; Fig. 6B, line b). Further addition of sodium dithionite to the AsA-reduced 4-PDS–treated cytochrome b_{561} caused an increase in the heme reduction level (Fig. 6B, line c), but it could not reach to the level of the control sample (Fig. 6C, line c). To clarify further the reaction with AsA, we conducted stopped-flow rapid-scan measurements.

Stopped-Flow Rapid-Scan Analyses—We showed previously that, upon mixing of oxidized cytochrome b_{561} with AsA, the entire time-course of the heme *b* reduction was very complicated due to the presence of two heme centers and the intramolecular electron transfer reactions but could be fitted with a linear combination of at least four exponential functions (*27*). Among the four exponentials, the fastest reduction phase was reasonably ascribed to the reduction of the heme center on the cytosolic side at higher than pH 6.5 (*27*).

Effects of the 4-PDS–treatment on the entire visible spectral change after the mixing with AsA (final concentrations; 1.0, 2.0, 4.0, and 8.0 mM) were first analyzed with the rapid-scan mode (exposure time, 1 ms per spectrum). However, a considerable part of the oxidized heme center was found to be reduced for both control and the 4-PDS–treated samples before the first spectrum was obtained after the mixing (mixing dead-time ~1.5 ms) (spectra not shown). This result indicated that the fast reduction phase of cytochrome b_{561} with AsA did not suffer so much even after the 4-PDS–treatment. However, it must be noted that the final reduction level of the two heme *b* centers was significantly lowered as described in a previous section (Fig. 6, A and B).

To evaluate the effect of the 4-PDS–treatment on the fast reduction phase of the heme *b* centers more precisely, the absorbance changes at 420 nm for the first 10 s were measured in a stopped-flow mode, and the traces were fitted with a combination of two single exponential functions {*i.e.*, $A_{420} = A_1 + A_2t + A_3\exp(-A_4t) + A_5\exp(-A_6t)$}. The traces were fitted well with the two single exponential functions without a significant contribution from the A_2 term (less than 5% of A_3 value) irrespective to the treatment with 4-PDS (spectra not shown). We focused on the apparent rate constant A_4, since this is most directly related the electron transfer rate from AsA to the oxidized heme center on the cytosolic side (*27*). The apparent rate constants were plotted against the final AsA concentrations, and the

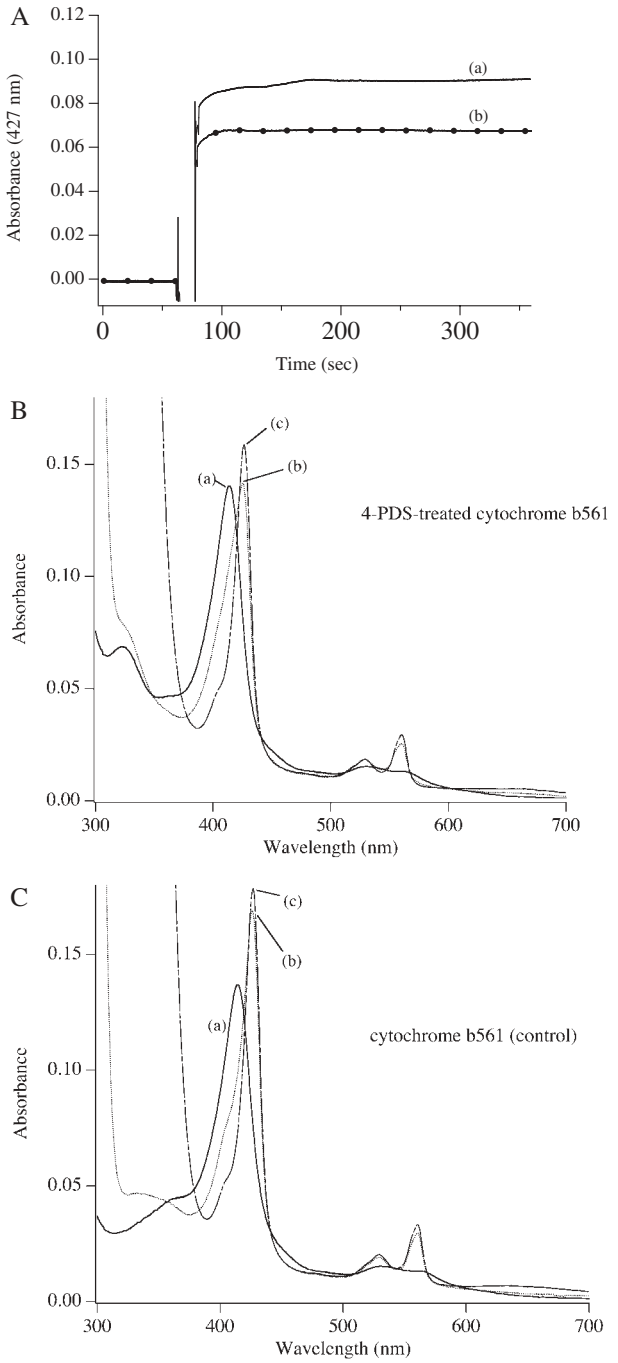

Fig. 6. **Time courses of the absorption changes at 427 nm upon reduction with 2 mM AsA of 4-PDS (40 μM)–treated sample or control sample of cytochrome b_{561} (panel A) and visible absorption spectra of the 4-PDS–treated (panel B) and control samples (panel C).** An optical quartz cell (light path, 1.0 cm) containing 1.0 ml of the control (trace a) or the 4-PDS (40 μM)–treated (trace b) oxidized cytochrome b_{561} [1.0 μM in 1.0% β-octyl glucoside, 50 mM sodium-phosphate buffer (pH 6.5)] was placed in a spectrophotometer. Twenty microliter of AsA solution (100 mM in the buffer) was added (final concentration, 2.0 mM) and the absorption change at 427 nm was recorded in the time-scan mode at 20°C for 30 min (panel A). Visible absorption spectra in panels B and C were measured in oxidized (trace a), AsA-reduced (trace b), and dithionite-reduced (trace c) states, respectively, for control (panel C) and the 4-PDS–treated (panel B) samples.

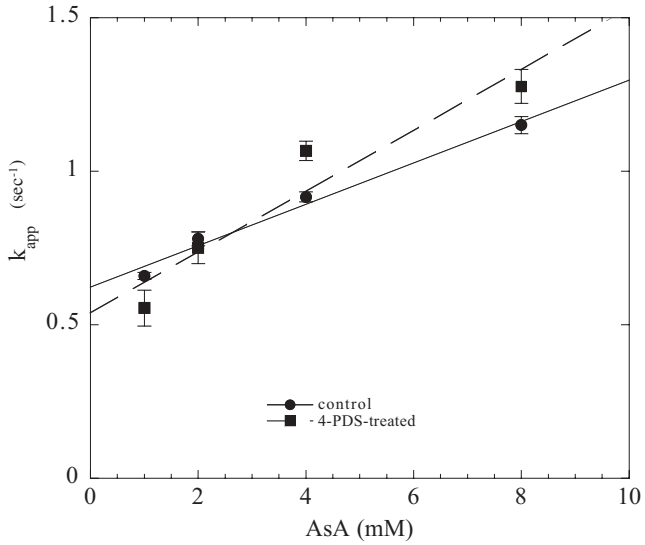

Fig. 7. **Concentration dependence of the apparent rate constants on the fast phase of the reaction of the 4-PDS–treated or control cytochrome b_{561} (final 1.0 μM) with AsA measured at pH 6.5.** The apparent rates for the fast phase were determined by the absorbance change at 427 nm in a stopped-flow mode (single wavelength mode), followed by the analyses as described in the text. The apparent rate constants for the fast phases were plotted against the final AsA concentrations and the first-order rate constants (k_{-1}, k_{+1}) were obtained under the assumption of an A + B ↔ C type bimolecular reaction. In the plots, intercepts indicate k_{-1}, whereas the slopes correspond to k_{+1}. The calculated k_{-1} and k_{+1} were 0.62 (s^{-1}) and 6.75×10^{-2} (s^{-1} mM^{-1}) for the control sample and 0.54 (s^{-1}) and 9.92×10^{-2} (s^{-1} mM^{-1}) for the 4-PDS–treated sample, respectively.

first-order rate constants were obtained under the assumption of an A + B ↔ C type bimolecular reaction (Fig. 7). As expected, there were no marked differences in either k_{-1} or k_{+1} between the two samples, suggesting that the 4-PDS–treatment did not affect the fast electron transfer reaction from AsA to the oxidized heme *b* center on the cytosolic side.

These results suggested that a part of the perturbed heme *b* center with 4-PDS could not be reduced at all, due to the local conformational change (partial denaturation?) around the heme moiety. To assess the extent of the conformational change caused by the 4-PDS treatment, we conducted EPR measurements.

EPR Spectra of 4-PDS–Treated Cytochrome b_{561}—As reported previously, oxidized cytochrome b_{561} showed two low-spin EPR signals at $g_z = 3.69$ and at $g_z = 3.14$ at cryogenic temperatures (*48*, *15*). The reactivity toward the DEPC-treatment and the different midpoint potential of these two EPR signals suggested that the heme species with $g_z = 3.69$ signal corresponds the cytosolic heme center and is responsible for the electron acceptance from cytosolic AsA, whereas the other species with $g_z = 3.14$ signal is likely the intravesicular heme center for the electron donation to the intravesicular MDA radical (*48*). In the spectra measured at 15 K, the $g_z = 3.14$ species dominated for the control sample (Fig. 8A, a). The 4-PDS–treatment caused a significant decrease in the signal intensity of the heme species with $g_z = 3.14$. Instead, a new signal around $g_z = 2.9$ appeared, and the intensity of the high-spin signal

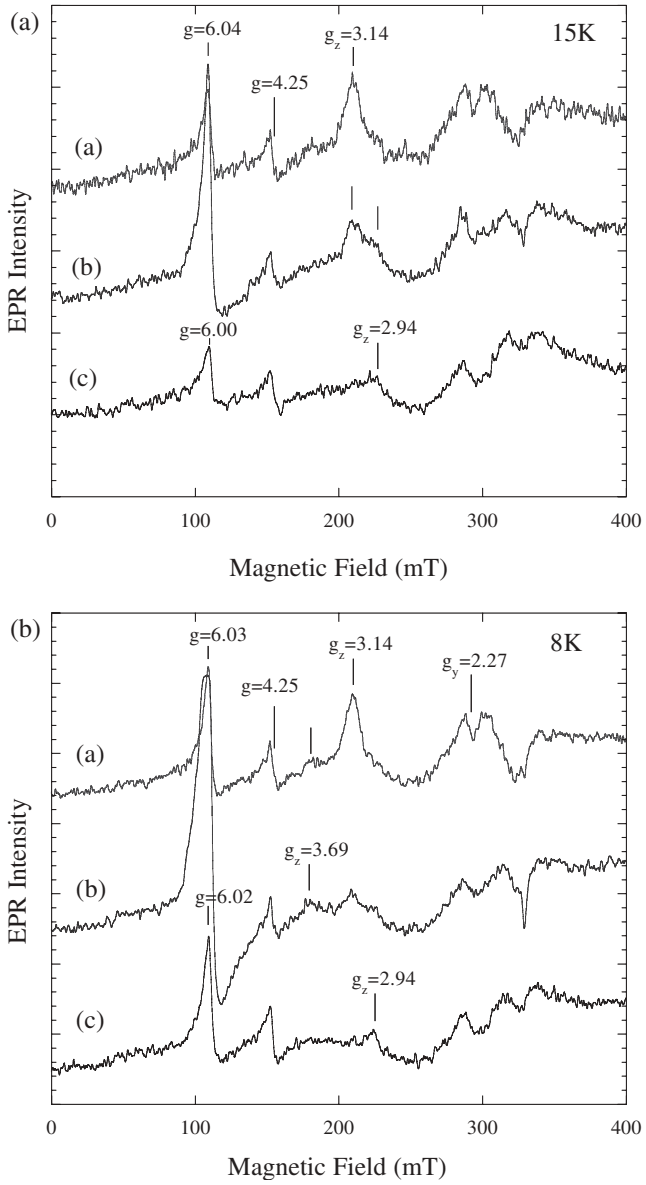

Fig. 8. **X-band EPR spectra of the 4-PDS–treated cytochrome b_{561} measured at 15 K (A) and 8 K (B).** In each panel, control (trace a), 4-PDS–treated in the oxidized form (trace b), and AsA (20 mM)-reduced form of the 4-PDS–treated (trace c) cytochrome b_{561} are shown. Other conditions are described in the text.

at g = 6.0 increased concomitantly (Fig. 8A, line b). In the spectra measured at 8 K (Fig. 8B, line b), such spectral changes were significantly pronounced. However, the g_z = 3.69 signal remained with almost the same intensity as that of the control sample after the 4-PDS–treatment (Fig. 8B, line b). Addition of AsA (final 20 mM) to the 4-PDS–treated cytochrome b_{561} caused the disappearance of both g_z = 3.14 and g_z = 3.69 signals and a significant decrease in intensity of the g = 6.0 high-spin signal (Fig. 8, A and B, line c). However, a low-spin signal remained at g_z = 2.94, which corresponds to the shoulder in the higher magnetic field of the g_z = 3.14 signal in the spectra of the oxidized 4-PDS–treated sample. This result was consistent with the inference obtained from the AsA-reactivity measurement that a part of the perturbed heme b center with 4-PDS could not be reduced by AsA due to a partial conformational change (denaturation?). Therefore, it could be concluded that the perturbed heme center was indeed on the intravesicular side, as expected.

DISCUSSION

Location of the Modification Sites with 4-PDS—There are two Cys residues (Cys57 and Cys125) in the mature form of bovine cytochrome b_{561} (Fig. 1). In a previous study conducted by Kent and Fleming (*49*), the number of the Cys residues in the mature form was erroneously considered as three. This discrepancy arouse because the initiation Met residue had not been defined conclusively at that time (*18*) and there was ambiguity about the covalent structure around the NH_2-terminal region (such as a possibility of covalent fatty acylation) (*49*). However, our recent study established the initiation Met residue and the acetylation of this Met residue based on the isolation of the NH_2-terminal peptide and its MALDI-TOF analysis (*50*). Our study concluded clearly that the Cys residue in the NH_2-terminal region does not exist in the mature form of bovine cytochrome b_{561}. Observation of the third Cys residue in the study conducted by Kent and Fleming might be due to the underestimation of cytochrome b_{561} concentration (*49*) caused by the partial loss of the heme prosthetic group during the purification procedure under mildly alkaline conditions (*22*, *51*).

Although the X-ray crystal structure of cytochrome b_{561} is not available at this stage, we could roughly image the three-dimensional structure of the cytochrome in the chromaffin vesicle membranes based on the six-transmembrane α-helices model (*22*). Asard and coworkers extended the model to include cytochrome b_{561} from various plants (*52*). According to the original and the extended models, both Cys57 and Cys125 locate inside of the transmembrane helices but very close to the fully-conserved His residues (His54 and His122; the potential His axial ligands of the intravesicular heme center), in each case with only two intervening amino acid residues (Fig. 2). This fact suggests that both Cys57 and Cys125 are located on the two adjacent α-helices, facing each other, and are very close to the heme prosthetic group on the intravesicular side if one considers that α-helices turn every 3.6 residues (Fig. 2). Although the environments around the Cys residues would be very hydrophobic (*40*), the lipophilic nature of 4-PDS can easily give access to these residues.

Reaction with 4-PDS—It is noteworthy that the reactivity toward 4-PDS was not greatly different between these two Cys residues (as shown as a single linear line in the semi-logarithmic scale plot of the release of 4-thiopyridone, Fig. 4A) and, as a result, only one 4-thiopyridine group was introduced per cytochrome b_{561} molecule. The space between the two Cys residues is probably not large enough to accommodate two 4-thiopyridine groups simultaneously (but large enough to prevent the formation of a disulfide -SS- bond) and, therefore, there were two populations having a 4-thiopyridine group, one at Cys57, and the other at Cys125. Since we could not detect mass peaks corresponding to the peptides having both Cys57 and

Cys125 modified with 4-PDS, the population of such species seemed very low, for the following reasons. (i) After the usual incubation time (5 h), the number of the modified Cys group was estimated as close to 1; (ii) The MALDI-TOF data indicated that the sample at this stage was a mixture of peptides having a Cys residue (either Cys57 or Cys125) being modified with 4-PDS and a free -SH group roughly in a 50:50 ratio; (iii) The number of the modified Cys groups estimated from the release of 4-thiopyridone groups was at most 1.6; but this high number was achieved only after a prolonged incubation.

Absence of the Effect of 4-PDS Treatment on the Reaction with AsA—Treatment of oxidized cytochrome b_{561} with 4-PDS did not cause any inhibition of the fast electron-accepting ability from AsA at all. This result is clearly shown in Fig. 4: upon mixing of oxidized cytochrome b_{561} with AsA, within the mixing time and the following several seconds, about a half of the oxidized heme centers were reduced. The same conclusion was drawn from our present stopped-flow and rapid-scan analyses on the reaction of AsA with the 4-PDS–treated cytochrome b_{561} (Fig. 7). These results were fully compatible with our structural and mechanistic model (*22*). The treatment of oxidized cytochrome b_{561} with 4-PDS did not have any influence on the heme center with g_z = 3.69 signal (Fig. 8). This result is consistent with our previous postulation that the heme center with g_z = 3.14 is located on the intravesicular side and responsible for the electron donation to MDA radical; whereas the heme center with g_z = 3.69 is responsible for the electron acceptance for the electron acceptance from AsA (*48*, *26*).

Effect of Cysteinyl-4-Thiopyridine Group on the Electronic Structure and the Redox Property of the Intravesicular Heme Center—Presence of a 4-thipyirdine (4-TP) group just beneath the porphyrin macrocyle would cause a significant perturbation on the electronic structure and the redox property of the intravesicular heme center. As expected, during the spectral measurements (in the difference spectra) after the addition of 4-PDS to the oxidized form of purified cytochrome b_{561}, there were two kinds of spectral changes occurring successively at the heme centers (Fig. 3): the first one was the "derivative-type" spectral change with a minimum at 425 nm and a maximum at 405 nm in the difference spectra, indicating the conversion from a low-spin species to a high-spin species, which appeared at the initial stage of the reaction; the second type subsequently showed a minimum at 422 nm in the difference spectra, but the maximum in the difference spectra became obscured, indicating the conversion of a low-spin heme center to a new perturbed state(s). The EPR results suggested that there were two kinds of new species being converted from the g_z = 3.14 low-spin heme species upon the 4-PDS treatment. One was the g = 6 high-spin species, which could be almost fully-reducible upon addition of AsA (Fig. 8). The other was the g = 2.94 species, which could not be reduced with AsA at all (Fig. 8).

Presence of two successive changes in the heme absorption spectra seemed inconsistent with the observation that there were no difference in the reactivity toward 4-PDS between Cys57 and Cys125. Therefore, it is likely that the formation of the g = 2.94 species (non-reducible form with AsA) was due to a secondary structural change being successively occurred on the g = 6 high-spin heme species formed by the 4-PDS treatment.

We had previously shown that the intravesicular heme center was very vulnerable to the changes of the medium, such as pH (*22*) or higher detergent concentration (Takeuchi *et al.*, unpublished). Incubation for only 30 min under mildly alkaline conditions (20°C) caused conversion of the g_z = 3.14 low-spin species to a new low-spin species with g_z = 2.84. This altered form also could not be reduced by AsA at all (*22*, *15*). Because of the close similarities in g_z values and in the non-reducibility with AsA, we consider that these two low-spin species (g_z = 2.94 and g_z = 2.84 species) have very similar properties. It is very interesting to note that a similar transition of EPR species occurred in cytochrome b_5, where a neutral form (g_z = 3.05) was converted to an alkaline form (g_z = 2.76) (*53*). The transition was ascribed either to deprotonation of one of the axial bisimdazole ligands to form an imidazolate or to an imidazole ligand becoming strongly hydrogen-bonded with a nearby amino acid residue (*54*).

Possible Roles of the Conservative Cysteinyl Residues—The presence of the two Cys residues (Cys57 and Cys125) very close to the intravesicular heme center is very interesting from the viewpoint of physiological functions, since these two Cys residues occur exclusively in neuroendocrine cytochrome b_{561} of higher vertebrates (Fig. 1) (*37*). These cytochromes have an established and clear role to donate an electron equivalent to the intravesicular MDA radical (*24*). To achieve such a specific role, the heme center has a relatively high redox potential (+155 mV) (*26*, *25*). Therefore, these two Cys residues, in combination with the coordinating His residues, may have a role to maintain the architecture around the heme prosthetic group suitable for such reactions. Alternatively, the two Cys residues may play a role to form a binding site for an MDA radical together with the well-conserved SLHSW sequence (*22*) (Fig. 2). It must be noted that *N*-carbethoxylation did not occur on the two coordinating imidazole groups (His54 and His122) of the intravesicular heme upon the treatment with DEPC, indicating that the environment of these heme-coordinating His ligands is somewhat unusual if we considered the high reactivity of DEPC towards ordinary His residues (*26*, *25*). The two Cys residues may protect these two His residues from modification by DEPC as a result of the formation of a specific network (hydrogen bonds) around the heme center. Further, such specific networks may have a role in the facilitated proton pathways to the MDA radical, because the electron donation to MDA radical from the reduced heme center must be coupled to the protonation of the MDA radical (*11*).

In conclusion, present study showed that the bound 4-thiopyridone at either Cys57 or Cys125 affected the electronic structure and properties of the intravesicular heme center of cytochrome b_{561}, converting the center to a non–AsA-reducible state. These results suggested the importance of the well-conserved two Cys residues near the intravesicular heme center and implied their physiological roles during the electron donation to the MDA radical. Further studies are necessary to clarify the structure and the operating mechanism at the crucial active center of cytochrome b_{561}.

REFERENCES

1. Eipper, B.A., Mains, R.E., and Glembotski, C.C. (1983) Identification in pituitary tissue of a peptide α-amidation activity that acts on glycine-extended peptides and requires molecular oxygen, copper, and ascorbic acid. *Proc. Natl. Acad. Sci. USA* **80**, 5144–5148
2. Eipper, B.A., Milgram, S.L., Husten, E.J., Yun, H., and Mains, R.E. (1993) Peptidylglycine α-amidating monooxgenase: A multifunctional protein with catalytic, processing, and routing domains. *Protein Science* **2**, 489–497
3. Kent, U.M. and Fleming, P.J. (1987) Purified cytochrome b_{561} catalyzes transmembrane electron transfer for dopamine β-hydroxylase and peptidyl glycine α-amidating monooxygenase activities in reconstituted systems. *J. Biol. Chem.* **262**, 8174–8178
4. Dhariwal, K.R., Black, C.D.V., and Lavine, M. (1991) Semidehydroascorbic acid as an intermediate in norepinephrine biosynthesis in chromaffin granules. *J. Biol. Chem.* **266**, 12908–12914
5. Njus, D., Kelley, P.M., and Harnadek, G.J. (1986) Bioenergetics of secretory vesicles. *Biochim. Biophys. Acta* **853**, 237–265
6. Njus, D., Knoth, J., Cook, C., and Kelley, P.M. (1983) Electron transfer across the chromaffin granule membrane. *J. Biol. Chem.* **258**, 27–30
7. Wakefield, L.M., Cass, A.E.G., and Radda, G.K. (1986) Functional coupling between enzymes of the chromaffin granule membrane. *J. Biol. Chem.* **261**, 9739–9745
8. Asada, A., Kusakawa, T., Orii, H., Agata, K., Watanabe, K., and Tsubaki, M. (2002) Planarian cytochrome b_{561}: Conservation of a six-transmembrane structure and localization along the central and peripheral nervous system. *J. Biochem.* **131**, 175–182
9. Duong, L.T., Fleming, P.J., and Russell, J.T. (1984) An identical cytochrome b_{561} is present in bovine adrenal chromaffin vesicles and posterior pituitary neurosecretory vesicles. *J. Biol. Chem.* **259**, 4885–4889
10. Pruss, R.M. and Shepard, E.A. (1987) Cytochrome b_{561} can be detected in many neuroendocrine tissues using a specific monoclonal antibody. *Neuroscience* **22**, 149–157
11. Njus, D. and Kelley, P.M. (1993) The secretory-vesicle ascorbate-regenerating system: a chain of concerted H^+/e^--transfer reactions. *Biochim. Biophys. Acta* **1144**, 235–248
12. Duong, L.T. and Fleming, P.J. (1982) Isolation and properties of cytochrome b_{561} from bovine adrenal chromaffin granules. *J. Biol. Chem.* **257**, 8561–8564
13. Silsand, T. and Flatmark, T. (1974) Purification of cytochrome *b*-561 An integral heme protein of the adrenal chromaffin granule membrane. *Biochim. Biophys. Acta* **359**, 257–266
14. Pruss, R.M. (1987) Monoclonal antibodies to chromaffin cells can distinguish proteins specific to or specifically excluded from chromaffin granules. *Neuroscience* **22**, 141–147
15. Tsubaki, M., Nakayama, M., Okuyama, E., Ichikawa, Y., and Hori, H. (1997) Existence of two heme B centers in cytochrome b_{561} from bovine adrenal chromaffin vesicles as revealed by a new purification procedure and EPR spectroscopy. *J. Biol. Chem.* **272**, 23206–23210
16. Burbaev, D.S., Moroz, I.A., Kamensky, Y.A., and Konstantinov, A.A. (1991) Several forms of chromaffin granule cytochrome *b*-561 revealed by EPR spectroscopy. *FEBS Lett.* **283**, 97–99
17. Liu, W., Kamensky, Y.A., Kakkar, R., Foley, E., Kulmacz, R.J., and Palmer, G. (2005) Purification and characterization of bovine adrenal cytochrome b_{561} expressed in insect and yeast cell systems. *Protein Expr. Purif.* **40**, 429–439
18. Perin, M.S., Fried, V.A., Slaughter, C.A., and Südhof, T.C. (1988) The structure of cytochrome b561, a secretory vesicle-specific electron transport protein. *EMBO J.* **7**, 2697–2703
19. Srivastava, M. (1996) *Xenopus* cytochrome b561: Molecular confirmation of a general five transmembrane structure and developmental regulation at the gastrula stage. *DNA Cell Biol.* **15**, 1075–1080
20. Srivastava, M., Gibson, K.R., Pollard, H.B., and Fleming, P.J. (1994) Human cytochrome b_{561}: A revised hypothesis for conformation in membranes which reconciles sequence and functional information. *Biochem. J.* **303**, 915–921
21. Srivastava, M., Pollard, H.B., and Fleming, P.J. (1998) Mouse cytochrome b561: cDNA cloning and expression in rat brain, mouse embryos, and human glioma cell lines. *DNA Cell Biol.* **17**, 771–777
22. Okuyama, E., Yamamoto, R., Ichikawa, Y., and Tsubaki, M. (1998) Structural basis for the electron transfer across the chromaffin vesicle membranes catalyzed by cytochrome b_{561}: Analyses of cDNA nucleotide sequences and visible absorption spectra. *Biochim. Biophys. Acta* **1383**, 269–278
23. Degli Esposti, M., Kamensky, Y.A., Arutjunjan, A.M., and Konstantinov, A.A. (1989) A model for the molecular organization of cytochrome b-561 in chromaffin granule membranes. *FEBS Lett.* **254**, 74–78
24. Kobayashi, K., Tsubaki, M., and Tagawa, S. (1998) Distinct roles of two heme centers for transmembrane electron transfer in cytochrome b_{561} from bovine adrenal chromaffin vesicles as revealed by pulse radiolysis. *J. Biol. Chem.* **273**, 16038–16042
25. Tsubaki, M., Kobayashi, K., Ichise, T., Takeuchi, F., and Tagawa, S. (2000) Diethylpyrocarbonate-modification abolishes fast electron accepting ability of cytochrome b_{561} from ascorbate but does not influence on electron donation to monodehydroascorbate radical: Distinct roles of two heme centers for electron transfer across the chromaffin vesicle membranes. *Biochemistry* **39**, 3276–3284
26. Takeuchi, F., Kobayashi, K., Tagawa, S., and Tsubaki, M. (2001) Ascorbate inhibits the carbethoxylation of two histidyl and one tyrosyl residues indispensable for the transmembrane electron transfer reaction of cytochrome b_{561}. *Biochemistry* **40**, 4067–4076
27. Takigami, T., Takeuchi, F., Nakagawa, M., Hase, T., and Tsubaki, M. (2003) Stopped-flow analyses on the reaction of ascorbate with cytochrome *b*561 purified from bovine chromaffin vesicle membranes. *Biochemistry* **42**, 8110–8118
28. Flatmark, T. and Terland, O. (1971) Cytochrome b_{561} of the bovine adrenal chromaffin granules. A high potential *b*-type cytochrome. *Biochim. Biophys. Acta* **253**, 487–491
29. Mckie, A.T., Barrow, D., Latunde-Dada, G.O., Rolfs, A., Sager, G., Mudaly, E., Mudaly, M., Richardson, C., Barlow, D., Bomford, A., Peters, T.J., Raja, K.B., Shirali, S., Hediger, M.A., Farzaneh, F., and Simpson, R.J. (2001) An iron-regulated ferric reductase associated with the absorption of dietary iron. *Science* **291**, 1755–1759
30. Mckie, A.T., Latunde-Dada, G.O., Miret, S., McGregor, J.A., Anderson, G.J., Vulpe, C.D., Wriggleworth, J.M., and Simpson, R.J. (2002) Molecular evidence for the role of a ferric reductase in iron transport. *Biochem. Soc. Trans.* **30**, 722–724
31. Escriou, V., Laporte, F., Garin, J., Brandolin, G., and Vignais, P.V. (1994) Purification and physical properties of a novel type of cytochrome *b* from rabbit peritoneal neutrophils. *J. Biol. Chem.* **269**, 14007–14014
32. Griesen, D., Su, D., Bérczi, A., and Asard, H. (2004) Localization of an ascorbate-reducible cytochrome b561 in the plant tonoplast. *Plant Physiol.* **134**, 726–734
33. Horemans, N., Foyer, C.H., and Asard, H. (2000) Transport and action of ascorbate at the plant plasma membrane. *Trends in Plant Science* **5**, 263–267
34. Preger, V., Scagliarini, S., Pupillo, P., and Trost, P. (2005) Identification of an ascorbate-dependent cytochrome *b* of the tonoplast membrane sharing biochemical features with members of the cytochrome *b*561 family. *Planta* **220**, 365–375

35. Trost, P., Bèrczi, A., Sparla, F., Sponza, G., Marzadori, B., Asard, H., and Pupillo, P. (2000) Purification of cytochrome b561 from bean hypocotyls plasma membrane. Evidence for the presence of two heme centers. *Biochim. Biophys. Acta* **1468**, 1–5
36. Ponting, C.P. (2001) Domain homologues of dopamine β-hydroxylase and ferric reductase: roles for iron metabolism in neurodegenerative disorders? *Hum. Mol. Genet.* **10**, 1853–1858
37. Tsubaki, M., Takeuchi, F., and Nakanishi, N. (2005) Cytochrome b561 protein family: Expanding roles and versatile transmembrane electron transfer abilities as predicted by a new classification system and protein sequence motif analyses. *Biochim. Biophys. Acta* (in press)
38. Tsubaki, M., Takigami, T., Seike, Y., and Takeuchi, F. (2003) Transmembrane electron transfer catalyzed by cytochrome b_{561}: Conserved properties and extending roles. *Recent Res. Devel. Biochem.* **4**, 39–52
39. Vargas, J.D., Herpers, B., Mckie, A.T., Gledhill, S., McDonnell, J., van der Heuvel, M., Davies, K.E., and Ponting, C.P. (2003) Stromal cell-derived receptor 2 and cytochrome *b*561 are functional ferric reductase. *Biochim. Biophys. Acta* **1651**, 116–123
40. Nagano, N., Ota, M., and Nishikawa, K. (1999) Strong hydrophobic nature of cysteine residues in proteins. *FEBS Lett.* **458**, 69–71
41. Dawson, J.H. (1988) Probing structure-function relations in heme-containing oxygenases and peroxidases. *Science* **240**, 433–439
42. Beinert, H., Holm, R.H., and Münck, E. (1997) Iron-sulfur clusters: Nature's modular, multipurpose structures. *Science* **277**, 653–659
43. Persson, A.L., Sahlin, M., and Sjöberg, B.-M. (1998) Cysteinyl and substrate radical formation in active site mutant E441Q of *Escherichia coli* class I ribonucleotide reductase. *J. Biol. Chem.* **273**, 31016–31020
44. Canaan, S., Riviére, M., Verger, R., and Dupis, L. (1999) The cysteine residues of recombinant human gastric lipase. *Biochem. Biophys. Res. Commun.* **257**, 851–854
45. Miller-Martini, D.M., Hua, S., and Horowitz, P.M. (1994) Cysteine 254 can cooperate with active site cysteine 247 in reactivation of 5′,5′-dithiobis(2-nitrobenzoic acid)-inactivated rhodanese as determined by site-directed mutagenesis. *J. Biol. Chem.* **269**, 12414–12416
46. Tsubaki, M., Tomita, S., Tsuneoka, Y., and Ichikawa, Y. (1986) Characterization of two cysteine residues in cytochrome P-450_{scc}: chemical identification of the heme-binding cysteine residue. *Biochim. Biophys. Acta* **870**, 564–574
47. Yep, A., Ballicora, M.A., Sivak, M.N., and Preiss, J. (2004) Identification and characterization of a critical region in the glycogen synthase from *Escherichia coli*. *J. Biol. Chem.* **279**, 8359–8367
48. Takeuchi, F., Hori, H., Obayashi, E., Shiro, Y., and Tsubaki, M. (2004) Properties of two distinct heme centers of cytochrome b_{561} from bovine chromaffin vesicles studied by EPR, resonance Raman, and ascorbate reduction assay. *J. Biochem.* **135**, 53–64
49. Kent, U.M. and Fleming, P.J. (1990) Cytochrome b561 is fatty acylated and oriented in the chromaffin granule membrane with its carboxyl terminus cytoplasmically exposed. *J. Biol. Chem.* **265**, 16422–16427
50. Nakamura, M., Takeuchi, F., and Tsubaki, M. (2003) Cytochrome b_{561} is not fatty acylated but acetylated at the amino terminus in the chromaffin vesicle membranes: An approach for identification of the posttranslational modification of transmembrane proteins. *Protoplasma* **221**, 41–46
51. Wanduragala, S., Wimalasena, D.S., Haines, D.C., Kahol, P.K., and Wimalasena, K. (2003) pH-Induced alteration and oxidative destruction of heme in purified chromaffin granule cytochrome b_{561}: Implications for the oxidative stress in catecholaminergic neurons. *Biochemistry* **42**, 3617–3626
52. Bashtovyy, D., Bérczi, A., Asard, H., and Páli, T. (2003) Structure prediction for the di-heme cytochrome b_{561} protein family. *Protoplasma* **221**, 31–40
53. Ikeda, M., Iizuka, T., Takao, H., and Hagihara, B. (1974) Studies on the heme environment of oxidized cytochrome b_5. *Biochim. Biophys. Acta* **336**, 15–24
54. Quinn, R., Nappa, M., and Valentine, J.S. (1982) New five- and six-coordinate imidazole and imidazolate complexes of ferric tetraphenylporphyrin. *J. Am. Chem. Soc.* **104**, 2588–2595